



# HOKKAIDO UNIVERSITY

Title	Transition from Liquid-solid to Liquid-liquid Surface Waves
Author(s)	TAZIME, Kyozi
Citation	Journal of the Faculty of Science, Hokkaido University. Series 7, Geophysics, 1(4), 301-314
Issue Date	1961-03-20
Doc URL	<a href="https://hdl.handle.net/2115/8643">https://hdl.handle.net/2115/8643</a>
Type	departmental bulletin paper
File Information	1(4)_p301-314.pdf



## Transition from Liquid-solid to Liquid-liquid Surface Waves

Kyozi TAZIME  
(Received Aug. 30, 1960)

### Abstract

Surface waves in a liquid layer over a solid bottom are investigated. There being complex roots in the characteristic equation, usual terminals of the dispersion curve have been extended from  $v_{s2}$  to  $v_{p2}$ . New waves here obtained seem to be incomplete surface waves.

### 1. Complex roots in the characteristic equation for liquid-liquid surface waves

If displacement potential of liquid waves is written as

$$\phi_j(t, x, z) \quad \text{where } j = 1 \text{ or } 2, \quad (1.1)$$

this must satisfy the next equation,

$$\partial^2 \phi_j / \partial t^2 = v_{pj}^2 \nabla^2 \phi_j. \quad (1.2)$$

If space-coordinates are taken as those illustrated in Fig. 1, (1.2) can have the following particular solution :

$$\phi_j = e^{i(\omega t - \xi x)} (A_j e^{i\alpha_j z} + B_j e^{-i\alpha_j z}) \quad (1.3)$$

where

$$\xi^2 + \alpha_j^2 = h_j^2 \quad \text{and} \quad h_j = \omega / v_{pj}. \quad (1.4)$$

Now several boundary conditions are given :

$$\left. \begin{array}{l} \text{normal stress must be zero at } z = 0 \\ \text{and} \\ \text{vertical displacements as well as normal stresses must be} \\ \text{continuous at } z = H. \end{array} \right\} (1.5)$$

Putting  $A_2 = 0$  in (1.3), the next relation will be obtained by the use of (1.5),

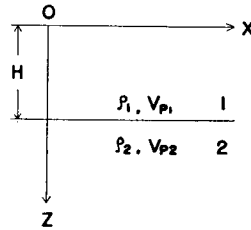


Fig. 1. Space-coordinates.

$$\tan \alpha_1 H = i (\rho_2/\rho_1)(\alpha_1/a_2) \quad (1.6)$$

which is the characteristic equation for liquid-liquid surface waves. By comparison of  $\phi_j$  in the present case with  $\psi_j$  in the previous one<sup>1)</sup>, it is seen that the characteristic equations are closely similar to each other.

If  $\omega$  is real as before<sup>1)</sup>,

$$\alpha_j \text{ must be } \pm (\bar{\alpha}_j + i \hat{\alpha}_j) \quad (1.7)$$

in the fourth quadrant on  $\xi$ -plane where  $\bar{\alpha}_j$  and  $\hat{\alpha}_j$  are real and positive.

Since

$$\left. \begin{aligned} \tan (\bar{\alpha}_1 + i \hat{\alpha}_1) H &= (\tan \bar{\alpha}_1 H \operatorname{sech}^2 \hat{\alpha}_1 H + i \tanh \hat{\alpha}_1 H \sec^2 \bar{\alpha}_1 H) \\ &\quad / (1 + \tan^2 \bar{\alpha}_1 H \tanh^2 \hat{\alpha}_1 H) \\ \text{and} \\ i (\bar{\alpha}_1 + i \hat{\alpha}_1) / (\bar{\alpha}_2 + i \hat{\alpha}_2) &= \{ \bar{\alpha}_1 \hat{\alpha}_2 - \hat{\alpha}_1 \bar{\alpha}_2 + i (\bar{\alpha}_1 \bar{\alpha}_2 + \hat{\alpha}_1 \hat{\alpha}_2) \} / (\bar{\alpha}_2^2 + \hat{\alpha}_2^2), \end{aligned} \right\} (1.8)$$

the characteristic equation can have no complex root, if

$$\alpha_2 = -(\bar{\alpha}_2 + i \hat{\alpha}_2). \quad (1.9)$$

Following the same procedure as before<sup>1)</sup> for finding complex roots, one will get

$$\left. \begin{aligned} P' &= (\rho_2/\rho_1)(R_{p1}/R_{p2}) \sin (\varepsilon_{p2} - \varepsilon_{p1}) \\ \text{and} \\ Q' &= (\rho_2/\rho_1)(R_{p1}/R_{p2}) \cos (\varepsilon_{p2} - \varepsilon_{p1}), \end{aligned} \right\} (1.10)$$

resulting in

$$\tan (\bar{\alpha}_1 + i \hat{\alpha}_1) H = P' + i Q'. \quad (1.11)$$

$\varepsilon_{pj}$  and  $R_{pj}$  correspond respectively to  $\varepsilon_j$  and  $R_j$  in the previous paper<sup>1)</sup> where they have already been illustrated in figures.

By means of the same treatment as before<sup>1)</sup>, complex roots may be found on  $\xi$ -plane. Details of the consideration are omitted here. When  $v_{p2}/v_{p1} > 1$ , however, no complex root can make predominant waves even if any wave will be born.

## 2. Expression of surface waves in a liquid layer over a solid bottom

Putting

$$A = -1, B = C = D = 0 \quad \text{and} \quad B' = C' = D' = 0 \quad (2.1)$$

in (1.23) and (1.24) of another previous paper<sup>2)</sup>, one will find in the present case that

$$\left. \begin{aligned} A_1 &= (A'e^{-2i\alpha_1 H} e^{i\alpha_1 E} - A'e^{-2i\alpha_1 H} e^{-i\alpha_1 E})/M \\ B_1 &= (-A'e^{-2i\alpha_1 H} e^{i\alpha_1 E} - e^{-i\alpha_1 E})/M \end{aligned} \right\} \quad (2.2)$$

and

$$\left. \begin{aligned} M &= 1 + A'e^{-2i\alpha_1 H} \\ M &= 1 + A'e^{-2i\alpha_1 H} = 0 \end{aligned} \right\} \quad (2.3)$$

is the characteristic equation for the present waves.

Operating  $\vartheta$  which has been defined before<sup>2)</sup> on  $M$ ,

$$[\vartheta M]_{M=0} = 2i\alpha_1 H. \quad (2.4)$$

Therefore the displacement potential of the present waves in the liquid layer will be expressed by

$$[\phi_1]_{M=0} = -\frac{2\pi\omega}{\alpha_1^2 H} \left( \frac{1}{U} - \frac{1}{c} \right) \sin \alpha_1 E \sin \alpha_1 z. \quad (2.5)$$

Reflecting coefficient  $A'$  in (2.3) is given by

$$\left. \begin{aligned} A' &= (Z-1)/(Z+1) \\ Z &= \left( \frac{\rho_2}{\rho_1} \right) \left( \frac{\alpha_1}{\alpha_2} \right) \left\{ \left( 1 - 2 \frac{v_{s2}^2}{c^2} \right)^2 + 4 \frac{\alpha_2}{\xi} \frac{\beta_2}{\xi} \left( \frac{v_{s2}}{c} \right)^4 \right\} \end{aligned} \right\} \quad (2.6)$$

in which

: By the use of (2.6), (2.3) can be rewritten as

$$\tan \alpha_1 H = iZ = i \left( \frac{\rho_2}{\rho_1} \right) \left( \frac{\alpha_1}{\alpha_2} \right) \left\{ \left( 1 - 2 \frac{v_{s2}^2}{c^2} \right)^2 + 4 \frac{\alpha_2}{\xi} \frac{\beta_2}{\xi} \left( \frac{v_{s2}}{c} \right)^4 \right\}. \quad (2.7)$$

Since  $Z$  of (2.6) was  $(\rho_2/\rho_1)(\alpha_1/\alpha_2)$  in the case described in the previous section, (2.7) will coincide with (1.6) for liquid-liquid waves if  $v_{s2}$  becomes just zero.

Now (2.7) can have real roots only when

$$\hat{\alpha}_1 = \bar{\alpha}_2 = \hat{\beta}_2 = 0. \quad (2.8)$$

Putting

$$\alpha_1 = \bar{\alpha}_1, \quad \alpha_2 = -i\hat{\alpha}_2 \quad \text{and} \quad \beta_2 = -i\hat{\beta}_2 \quad (2.9)$$

in (2.7), one has

$$\tan \bar{\alpha}_1 H = - \left( \frac{\rho_2}{\rho_1} \right) \left( \frac{\bar{\alpha}_1}{\hat{\alpha}_2} \right) \left\{ \left( 1 - 2 \frac{v_{s2}^2}{c^2} \right)^2 - 4 \frac{\hat{\alpha}_2}{\xi} \frac{\hat{\beta}_2}{\xi} \left( \frac{v_{s2}}{c} \right)^4 \right\} \quad (2.10)$$

which is the same expression as that given already by EWING et al.<sup>3)</sup>

### 3. Organization of the dispersion curve

From now on

$$\rho_2/\rho_1 = 1 \tag{3.1}$$

will be assumed, for simplicity, in the present paper.

In order to get the dispersion curve, the next formula can be obtained from (2.10),

$$T v_{p1}/H = 2 \pi \{ 1 - (v_{p1}/c)^2 \}^{1/2} / (\tan^{-1} \hat{Z} + l\pi) \tag{3.2}$$

where  $\hat{Z} = iZ$  and  $l$  means any integer.

Several dispersion curves are shown in Fig. 2 with thick lines where  $v_{p2}/v_{p1} = 10$  and POISSON'S ratio  $\sigma_2$  in the bottom is assumed to be 0.25. The numbers in parentheses in Fig. 2 indicate the order of the solution.

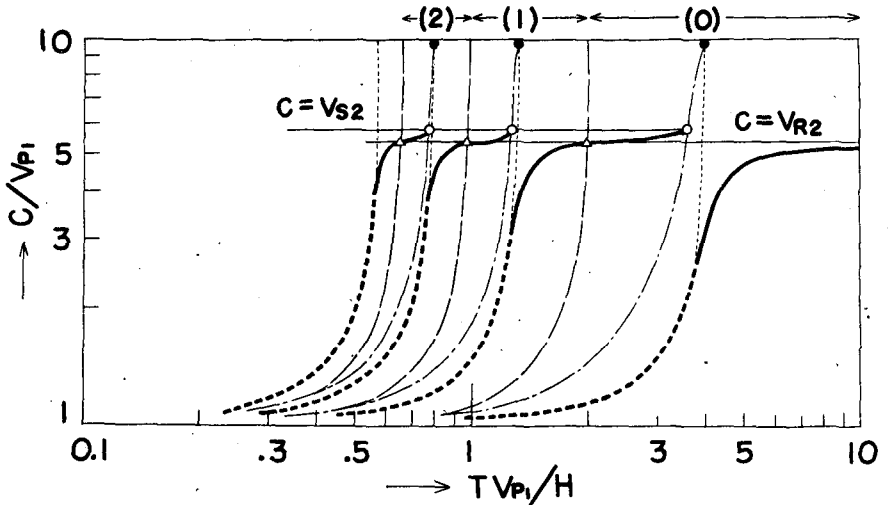


Fig. 2. Dispersion curves when  $v_{p2}/v_{p1} = 10$  and  $\sigma_2 = 0.25$ .

If  $v_{p2}/v_{p1} \rightarrow \infty$  otherwise  $c = v_{p2}$ , the absolute value of the right hand side in (2.10) becomes extremely larger than unity. Thus (2.10) will be reduced to

$$\cos \bar{\alpha}_1 H = 0 \quad \text{when } v_{p2}/v_{p1} \gg 1 \text{ otherwise } c = v_{p2} \tag{3.3}$$

which is shown with dotted lines. Intersecting points of these with  $c = v_{p2}$  are marked with •.

If the value in braces of the right hand side in (2.10) is zero, velocity of RAYLEIGH waves as to the bottom will be obtained and (2.10) will be reduced at the same time to

$$\sin \bar{\alpha}_1 H = 0 \quad \text{when } c = v_{R2} \quad (3.4)$$

which is shown with broken lines. Intersecting points of these with  $c=v_{R2}$  are marked with  $\Delta$ .

If  $v_{s2}$  becomes just zero otherwise  $c=v_{s2}$ , (2.10) will be reduced to (1.6) which is shown with chain lines. Intersecting points of these with  $c=v_{s2}$  are marked with  $\circ$  in Fig. 2.

It must be noticed in (2.10) that

$$\left(1 - 2 \frac{v_{s2}^2}{c^2}\right)^2 - 4 \frac{\alpha_2}{\xi} \frac{\beta_2}{\xi} \left(\frac{v_{s2}}{c}\right)^4 \leq 0 \quad \text{for } c \leq v_{R2}, \quad (3.5)$$

that is in (3.2)

$$l = \begin{cases} n \\ n - 1 \end{cases} \quad \text{for } c \leq v_{R2} \quad (3.6)$$

in which  $n$  means 0, 1, 2, ..., and indicates the number of nodes of amplitude distribution in the superficial layer. Therefore the order  $l$  of the solution does not always coincide with the number  $n$  of nodes throughout one dispersion curve. In order to avoid this confusion, the order as well as the number must be bordered by (3.4), as shown in Fig. 2.

One dispersion curve is formed in general from two parts. One starts from  $c=v_{p1}$  along (3.3) as far as  $c/v_{p1}$  has not much larger value than unity, then it approaches gradually to  $c=v_{R2}$ , terminating at  $\Delta$ . The other starts from  $\Delta$  and leaves  $c=v_{R2}$  gradually, then reaches  $\circ$ .

Letting  $\sigma_2$  change from 0.25 to 0.48, one will see that  $\circ$  for  $\sigma_2 = 0.25$  goes down along a chain line until  $\circ$  for  $\sigma_2 = 0.48$ , as shown by Fig. 3. No real root exists between  $\circ$  for  $\sigma_2 = 0.48$  and  $\bullet$ , as it was.

If  $\sigma_2$  increases more and more until the limit, 0.50,  $\circ$  corresponding to it will disappear from Fig. 3. In other words, (2.10) can have no real root other than that at  $\bullet$  if  $v_{s2}$  is very small but different from zero.

However this is physically too curious to be recognized, because (2.10) must be reduced to (1.6) and real roots are shown with chain lines when  $v_{s2}=0$ . It will be expected, therefore, that (1.6) may be satisfied approximately in the neighbourhood of  $c=v_{p2}$  even if  $c$  does not coincide exactly with  $v_{p2}$  and the approximation will be the better, the larger  $c/v_{p1}$ .

For the purpose of removing the physical difficulty from (2.10) and of

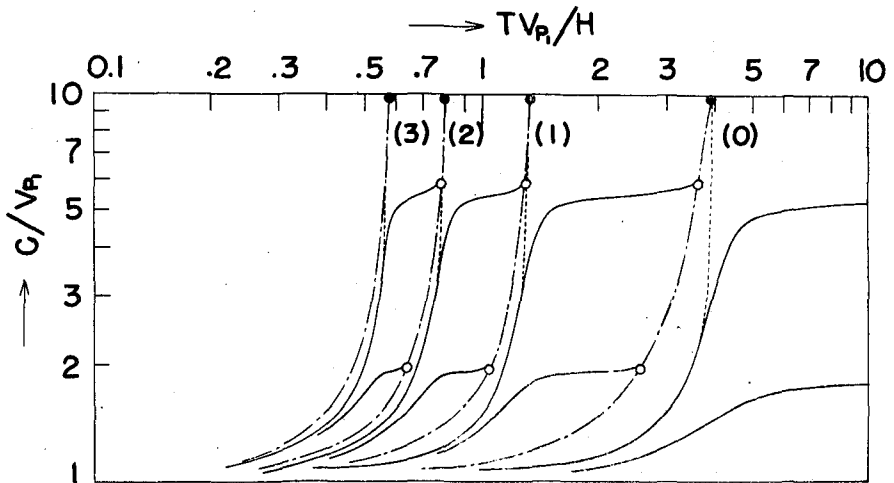


Fig. 3. Comparison of dispersion curves for  $\sigma_2=0.25$  with those for  $\sigma_2=0.48$  when  $v_{p2}/v_{p1}=10$ .

ascertaining the above expectation in practice, complex roots must be found in (2.7).

#### 4. Complex roots in the characteristic equation for surface waves in a liquid layer over a solid bottom

Putting

$$P'' + iQ'' = \left(1 - 2\frac{v_{s2}^2}{c^2}\right)^2 + 4\frac{\alpha_2}{\xi} \frac{\beta_2}{\xi} \left(\frac{v_{s2}}{c}\right)^4, \quad (4.1)$$

(2.7) will be expressed as

$$\tan \alpha_1 H = P + iQ \quad (4.2)$$

in which

$$P = P'P'' - Q'Q'' \quad \text{and} \quad Q = P'Q'' + Q'P'', \quad (4.3)$$

using (1.10) where

$$\alpha_2 = \bar{\alpha}_2 + i\hat{\alpha}_2 \quad (4.4)$$

was assumed.

In the case of liquid-liquid,  $Q'$  should be positive and (1.9) was omitted from further consideration. In the present case, however, not  $Q'$  but  $Q$  must be positive. Thus (1.9) can not always be omitted.

Various combinations of  $\alpha_2$ ,  $\beta_2$  and  $\alpha_1$  will be considered here, as tabulated in Table 1. But (2.7) will not be disturbed by putting (iv) in place of (iii) and the brace in (2.7) by putting (iii) in place of (i). Therefore there is no distinction between (iii) and (iv) as long as (2.7) is concerned.

Table 1.

(i)	$\bar{\alpha}_2 + i \hat{\alpha}_2,$	$\bar{\beta}_2 + i \hat{\beta}_2,$	$\bar{\alpha}_1 + i \hat{\alpha}_1,$
(ii)	$-(\bar{\alpha}_2 + i \hat{\alpha}_2),$	$\bar{\beta}_2 + i \hat{\beta}_2,$	$\bar{\alpha}_1 + i \hat{\alpha}_1,$
(iii)	$-(\bar{\alpha}_2 + i \hat{\alpha}_2),$	$-(\bar{\beta}_2 + i \hat{\beta}_2),$	$\bar{\alpha}_1 + i \hat{\alpha}_1,$
(iv)	$-(\bar{\alpha}_2 + i \hat{\alpha}_2),$	$-(\bar{\beta}_2 + i \hat{\beta}_2),$	$-(\bar{\alpha}_1 + i \hat{\alpha}_1).$

When  $v_{p2}/v_{p1} > 1$ ,  $\epsilon_{p2}$  is always larger than  $\epsilon_{p1}$  as to the same  $\hat{c}/\bar{c}$ . Thus both  $P'$  and  $Q'$  are positive in (i). In (ii) and (iii), on the contrary, they must be replaced by  $-P'$  and  $-Q'$  respectively in (4.3). Therefore Table 2 is prepared for numerical calculations.

Table 2.

(i)	$P = P'P'' - Q'Q'',$	$Q = P'Q'' + Q'P'',$
	$P'' = \text{Re } p + \text{Re } q,$	$Q'' = \text{Im } p + \text{Im } q.$
(ii)	$P = -(P'P'' - Q'Q''),$	$Q = -(P'Q'' + Q'P''),$
	$P'' = \text{Re } p - \text{Re } q,$	$Q'' = \text{Im } p - \text{Im } q.$
(iii)	$P = -(P'P'' - Q'Q''),$	$Q = -(P'Q'' + Q'P''),$
	$P'' = \text{Re } p + \text{Re } q,$	$Q'' = \text{Im } p + \text{Im } q.$

By the use of figures of  $\epsilon_j$  and  $R_j$  in the previous paper<sup>1</sup>),  $P'$  and  $Q'$  can be easily calculated from formula (1.10). On the other hand,  $p$  and  $q$  are expressed as follows :

$$\left. \begin{aligned} \text{Re } p &= 1 - 4 (v_{s2}/\bar{c})^2 \cos^2 \delta \{ \cos 2 \delta - (v_{s2}/\bar{c})^2 \cos^2 \delta \cos 4 \delta \}, \\ \text{Im } p &= 4 (v_{s2}/\bar{c})^2 \cos^2 \delta \{ \sin 2 \delta - (v_{s2}/\bar{c})^2 \cos^2 \delta \sin 4 \delta \}, \\ \text{Re } q &= 4 (v_{s2}/\bar{c})^4 R_{p2} R_{s2} \cos^2 \delta \cos (\epsilon_{p2} + \epsilon_{s2} - 2 \delta), \\ \text{Im } q &= 4 (v_{s2}/\bar{c})^4 R_{p2} R_{s2} \cos^2 \delta \sin (\epsilon_{p2} + \epsilon_{s2} - 2 \delta), \end{aligned} \right\} (4.5)$$

where

$$\delta = \tan^{-1} (\hat{c}/\bar{c}). \tag{4.6}$$

Then, from (4.2), one has

$$\tan 2\bar{\alpha}_1 H = 2P/(1-P^2-Q^2) \quad \text{and} \quad \tanh 2\hat{\alpha}_1 H = 2Q/(1+P^2+Q^2). \tag{4.7}$$

Eliminating  $\omega$  from (4.7), one obtains

$$\tan \epsilon_{p1} = \hat{\alpha}_1/\bar{\alpha}_1 = \tanh^{-1} \{ 2Q/(1+P^2+Q^2) \} / \tan^{-1} \{ 2P/(1-P^2-Q^2) \}. \tag{4.8}$$

Corresponding frequencies to the root of (4.8) will be obtained from

$$\omega H/v_{p1} = (\bar{c}/v_{p1}) \tan^{-1} \{ 2P/(1-P^2-Q^2) \} / (2R_{p1} \cos \epsilon_{p1}). \tag{4.9}$$

As has been seen before<sup>1</sup>),

$$\left. \begin{aligned} \tan^{-1} \{ 2P/(1-P^2-Q^2) \} &= \text{Tan}^{-1} \{ 2P/(1-P^2-Q^2) \} + (2n+1)\pi \\ &\text{for } \tan \bar{\alpha}_1 H \tan 2\bar{\alpha}_1 H < 0 \end{aligned} \right\}$$

and 
$$\tan^{-1} \left\{ \frac{2P}{1-P^2-Q^2} \right\} = \text{Tan}^{-1} \left\{ \frac{2P}{1-P^2-Q^2} \right\} + 2n\pi \quad \left. \vphantom{\tan^{-1}} \right\} (4.10)$$

for  $\tan \bar{\alpha}_1 H \tan 2 \bar{\alpha}_1 H > 0$ .

**5. Results of numerical calculations**

For various  $\hat{c}/\bar{c}$  numerical calculations of  $p$  and  $q$  were made, the parameter being  $\bar{c}/v_{p1}$ . Though these calculations are not shown here,  $Q$  in (i) has been found positive for any  $\bar{c}/v_{p1}$ . Therefore  $Q$  in (iii) should be negative and (4.7) cannot be satisfied by (iii). On the other hand,  $Q$  in (ii) can be positive sometimes within the region  $v_{s2} < c < v_{p2}$ .

Loci of complex roots found from (4.8) are illustrated by thick dotted lines for (ii) and by thick broken lines for (i) in Fig. 4 where  $v_{p2}/v_{p1}=10$  and  $\sigma_2=0.48$ . These broken lines correspond to loci of complex roots in the characteristic equation for LOVE type waves and for liquid-liquid surface waves. Complex roots on these broken lines, since they cannot develop predominant waves for the same reason as stated before<sup>1)</sup>, will be neglected after here.

Complex roots on the thick dotted lines have appeared for the first time in the present case. They seem to be important, because  $\hat{c}/\bar{c}$  may be very small in the neighbourhood of  $h_2$ . The thick full line in Fig. 4 is the locus of usual real roots. One sees that the thick full and dotted lines touch each other at  $k_2$ .

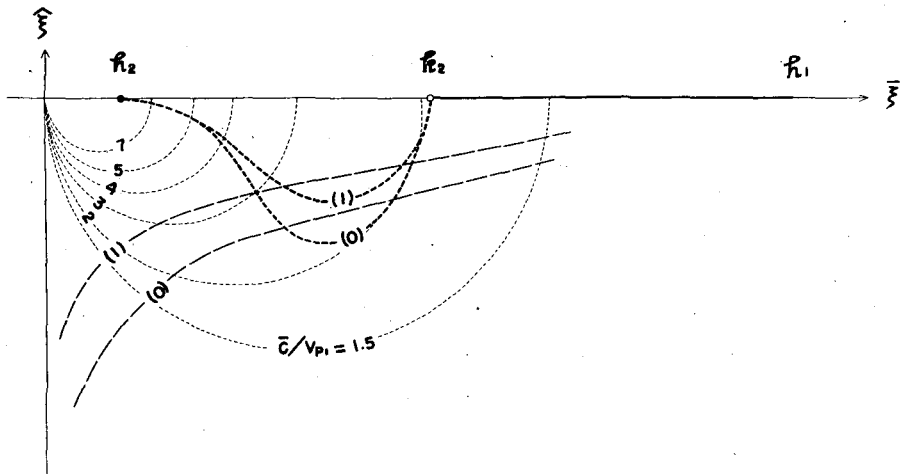


Fig. 4. Loci of complex roots when  $v_{p2}/v_{p1}=10$  and  $\sigma_2=0.48$ .

Complex roots of the zeroth order for the other  $\sigma_2$  have been obtained merely by combination (ii) and are illustrated in Fig. 5.

Relation between  $\bar{c}/v_{p1}$  and  $Tv_{p1}/H$  have also been calculated with (4.9). They are shown in Fig. 6 where full lines indicate the parts from real roots, dotted lines do the parts from complex roots and chain lines are the dispersion curves for liquid-liquid surface waves.

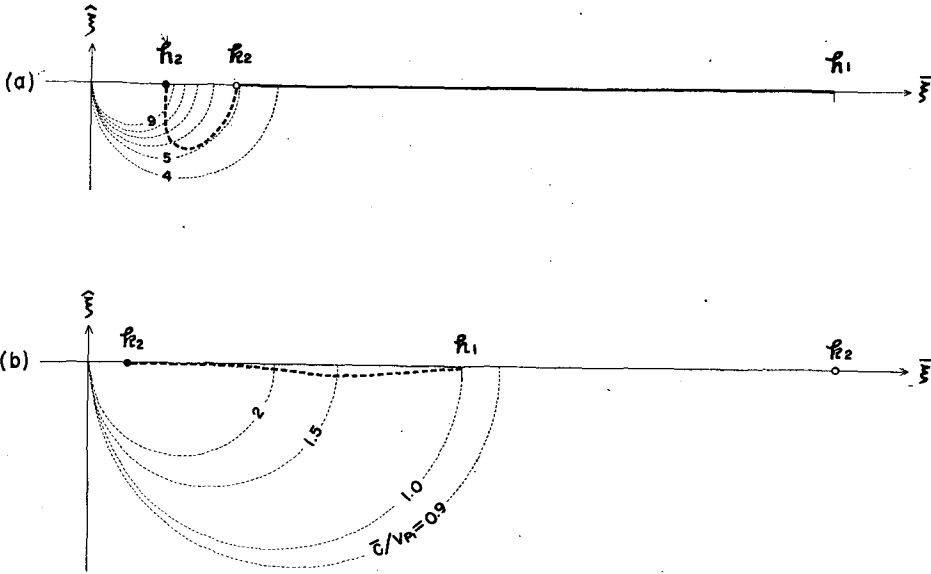


Fig. 5. Loci of complex roots of the zeroth order when  $v_{p2}/v_{p1}=10$  and (a)  $\sigma_2=0.25$  and (b)  $v_{p2}/v_{s2}=20$ .

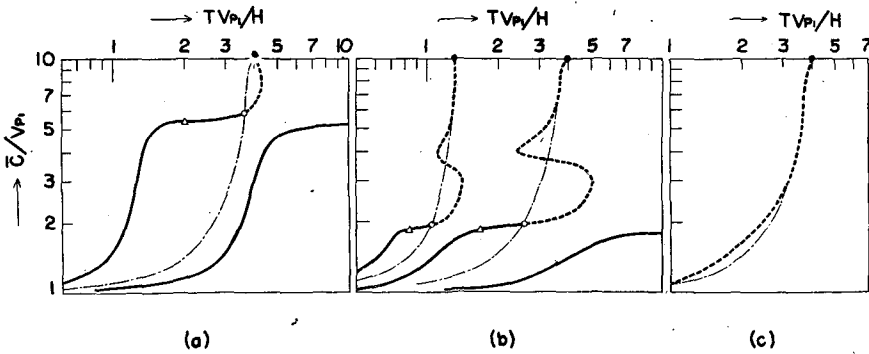


Fig. 6. Relation between  $\bar{c}/v_{p1}$  and  $Tv_{p1}/H$  when  $v_{p2}/v_{p1}=10$  and (a)  $\sigma_2=0.25$ , (b)  $\sigma_2=0.48$  and (c)  $v_{p2}/v_{s2}=20$ .

As it has been expected physically, these figures show that the larger part of the dotted line will coincide with the chain one if  $\sigma_2$  becomes nearer to 0.50. This is the numerical recognition, by means of dispersion curves, of transition from liquid-solid to liquid-liquid surface waves.

### 6. Difference of the boundary condition for liquid-solid from that for liquid-liquid

Tangential stress in the solid bottom can be expressed as

$$(\Psi_{zx})_2 = \mu_2(\partial u_2/\partial z + \partial w_2/\partial x), \quad (6.1)$$

denoting horizontal and vertical displacements respectively by  $u_2$  and  $w_2$ .

In the case of liquid-solid, one has used the condition

$$\partial u_2/\partial z + \partial w_2/\partial x = 0 \quad \text{at } z = H, \quad (6.2)$$

for the purpose of making

$$(\Psi_{zx})_2 = 0. \quad (6.3)$$

In the case of liquid-liquid, on the other hand,  $\mu_2 = 0$  and (6.3) is always satisfied if shearing strain is not zero. Indeed this is the definite difference between (1.6) and (2.7), but shearing strain in the case of liquid-liquid is expressed as  $-2\xi\alpha_2 B_2 \exp(-i\alpha_2 z)$  which becomes zero if  $\alpha_2 = 0$ . Therefore (6.2) may be also satisfied by liquid-liquid surface waves in the neighbourhood of  $c = v_{p2}$ . This should be the reason why the dotted line will coincide with the chain line at or near  $c = v_{p2}$  in Fig. 6. If  $\mu_2$  becomes very small, (6.3) does not need (6.2), resulting in the coincidence of the dotted line with the chain one.

The above consideration will be confirmed by the investigation of reflecting coefficient  $A'$  which is calculated with real  $c$  alone and is illustrated in Fig. 7 where  $A' = -|A'| \exp(2i\delta')$  between  $v_{p1} < c < v_{p2}$ .

In the region  $v_{p2} < c$ ,  $A'$  has nearly equal value for various  $\sigma_2$ .

In the region  $v_{s2} < c < v_{p2}$ , the absolute value as well as the phase lag for  $\sigma_2 = 0.50$  are different from those of the other  $\sigma_2$ : However both differences become smaller and smaller in the neighbourhood of  $c = v_{p2}$  when  $\sigma_2$  approaches to 0.50.

In the region  $v_{p1} < c < v_{s2}$ , each absolute value becomes unity but the phase lag is different to each other  $\sigma_2$ .

In the region  $c < v_{p1}$ ,  $A'$  for  $\sigma_2 = 0.50$  has entirely different value from the other  $\sigma_2$ .

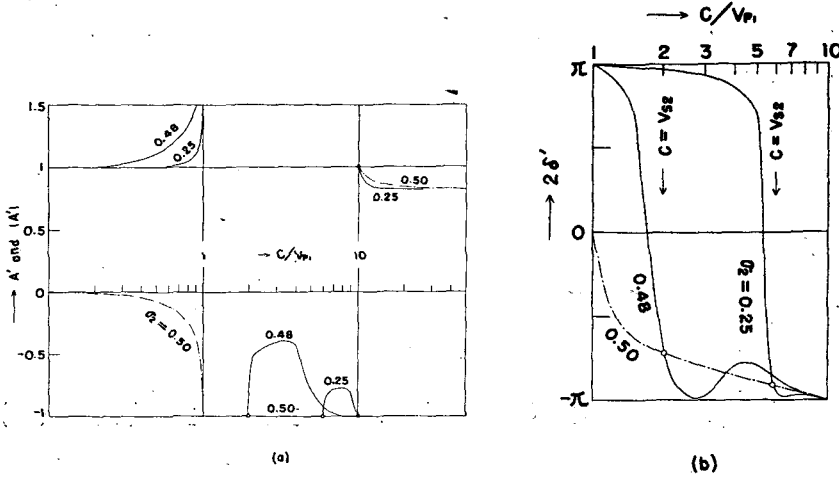


Fig. 7. PP-reflecting coefficient  $A'$  for various values of  $\sigma_2$  when  $v_{p2}/v_{p1}=10$ .

The further  $c$  removes from  $v_{p2}$ , the more difference must appear between the conditions (6.2) and  $\mu_2=0$ .

7. RIEMANN sheets

It has been found as described above in the previous section that the characteristic equation (2.7) has complex roots. However it must be another matter whether any wave will be developed or not, due to these roots.

In order to investigate this question, the locus of roots should be laid upon RIEMANN sheets.

If SOMMERFERD'S branch line is adopted, the permissible RIEMANN sheet<sup>3)</sup> will become as shown in Fig. 8 where the combination of wave numbers

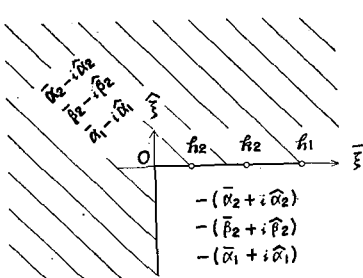


Fig. 8. The permissible RIEMANN sheet after SOMMERFERD.

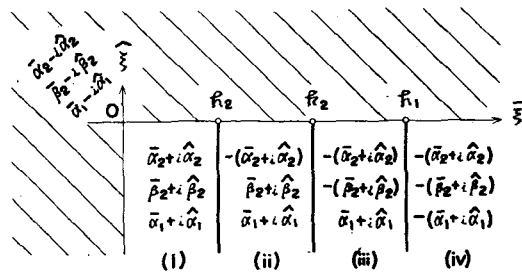


Fig. 9. The permissible RIEMANN sheet after LAMB.

in  $z$ -direction corresponds to (iv) in Table 1 everywhere in the fourth quadrant on  $\xi$ -plane. No important locus of complex roots, for example thick dotted lines in Fig. 4, exist on this sheet.

If LAMB's branch line is adopted, the permissible RIEMANN sheet will become as shown in Fig. 9. This means, important loci of complex roots exist in the domain denoted by (ii) and the locus of real roots exists on the real axis from  $h_2$  to  $h_1$ .

When the line integral as to displacement potential is made on the permissible RIEMANN sheet after LAMB, considerable residues will be obtained also from complex roots in domain (ii), besides those from real roots.

Looking back at the expression of displacement potentials,

$$\phi_2 \propto \exp(-\hat{\alpha}_2 z) \exp(i\hat{\alpha}_2 z) \quad \text{and} \quad \psi_2 \propto \exp(\hat{\beta}_2 z) \exp(-i\hat{\beta}_2 z) \quad (7.1)$$

in domain (ii). It seems very curious that  $\phi_2$  should regress in  $z$ -direction and  $\psi_2$  should increase its amplitude in  $z$ -direction.

When  $v_{p2}/v_{p1}=10$  and  $\sigma_2=0.48$ , however,

$$\bar{c}/v_{p2} = 0.7 \quad \text{and} \quad \bar{c}/v_{s2} = 3.6 \quad \text{for} \quad \bar{c}/v_{p1} = 7$$

and it will be found, using the relation<sup>1)</sup> between  $\tan \epsilon_j$  and  $\hat{c}/\bar{c}$  that

$$\hat{\alpha}_2/\bar{\alpha}_2 = 10, \quad \hat{\beta}_2/\bar{\beta}_2 = 0.003 \quad \text{and} \quad \hat{\alpha}_1/\bar{\alpha}_1 = 0.001$$

for  $\hat{c}/\bar{c}=0.046$  which is gotten, corresponding to  $\bar{c}/v_{p1}=7$ , from the locus of complex roots on  $\xi$ -plane.

Therefore the next approximation may be allowed in practice.

$$\alpha_2 \approx -i\hat{\alpha}_2, \quad \beta_2 \approx \bar{\beta}_2 \quad \text{and} \quad \alpha_1 \approx \bar{\alpha}_1 \quad \text{if} \quad \bar{c} \approx v_{p2}. \quad (7.2)$$

This means that incomplete surface waves may be developed, because

$$\phi_2 \propto \exp(-\hat{\alpha}_2 z) \quad \text{and} \quad \psi_2 \propto \exp(-i\bar{\beta}_2 z). \quad (7.3)$$

Some energy must escape as S waves, though no energy does as P waves into the bottom. The present author expects these incomplete surface waves occur not only in liquid-solid layers investigated here but also in solid-solid ones.

## 8. Group velocity and amplitude function

Corresponding to phase velocity from real roots, group velocity and amplitude function are illustrated in Figs. 10 and 11 with thick lines for the zeroth order and with thin lines for the first order. As in the case of phase

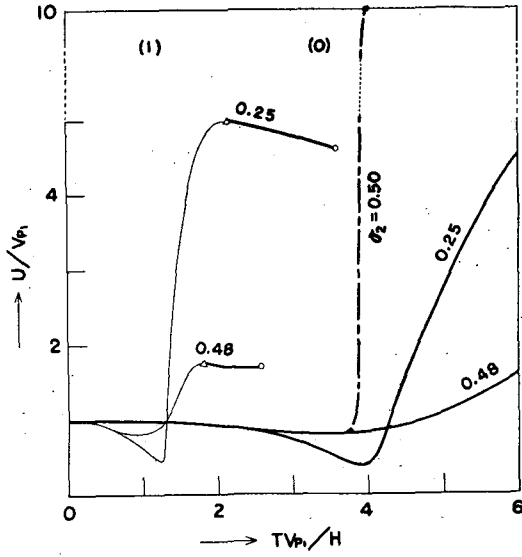


Fig. 10. Group velocity when  $v_{p2}/v_{p1}=10$ .

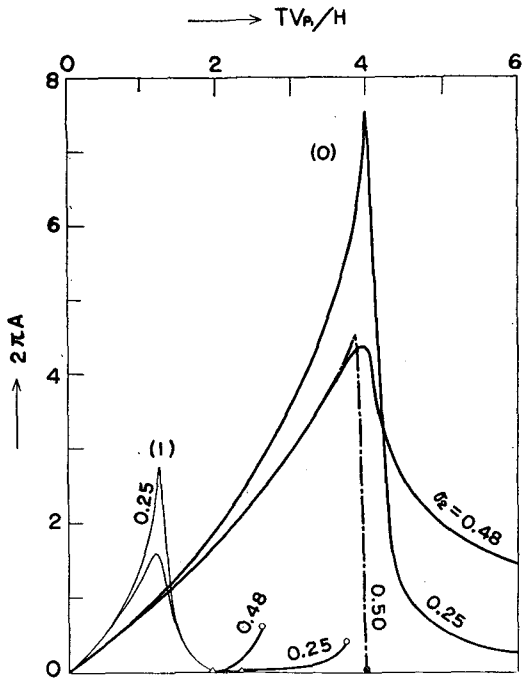


Fig. 11. Amplitude function when  $v_{p2}/v_{p1}=10$ .

velocity,  $\circ$  in these figures is to be connected to  $\bullet$  with a complicated line obtained from complex roots.

It must be noticed here that there might be two maxima of amplitude function near  $T v_{p1}/H=4$ : one is the peak shown by the full line and the other the peak which may be shown approximately by the chain line. In practice, therefore, two predominant phases may be observed by chance with one period, for instance  $T v_{p1}/H=4$ . They must be each distinguished from group and phase velocities.

Sometimes a large and regular phase is observed which has phase and group velocities similar to the velocity of P waves in the bottom. This might be the new waves under discussion. However numerical examples in the present paper have been investigated for too large  $v_{p2}/v_{p1}$  to be compared with usual structure of the earth. For the sake of recognizing qualitative features of complex roots,  $v_{p2}/v_{p1}=10$  has been adopted in the present paper.

*Acknowledgements* The author expresses his thanks to Prof. Takeo MATUZAWA for instructive discussions on the boundary condition. The author is indebted also to Miss Miyako MUROTA for her help in numerical calculations.

#### References

- 1) TAZIME, K.: Complex Roots in the Characteristic Equation for LOVE-type Waves in a Layer over a Half Space. Journ. Fac. Sci. Hokkaido Univ. VII, **1** (1960), 283-300.
- 2) TAZIME, K.: Ray-theoretical Construction of Dispersive RAYLEIGH Waves. Journ. Phys. Earth, **6** (1958), 81-89.
- 3) EWING, JARDETZKY and PRESS: Elastic Waves in Layered Media. MCGRAW-HILL, 1957.